RESEARCH PAPER

pH-sensitive thiolated nanoparticles facilitate the oral delivery of insulin in vitro and in vivo

**Yan Zhang · Xia Lin · Xuli Du · Sicong Geng ·
Hongren Li · Hong Sun · Xing Tang ·
Wei Xiao**

Abstract In this work, we designed and developed a delivery system composed of enteric Eudragit L100-cysteine/reduced glutathione nanoparticles (Eul-cys/GSH NPs) for oral delivery of insulin. First, interactions between Eul-cys and mucin glycoproteins, which are believed to be the result of disulfide bonds, were confirmed using rheology experiments. Subsequently, the insulin-loaded Eul-cys/GSH NPs were prepared by the diffusion method using the rich gel network multipore structure at the surface of the Eul-cys when the pH was higher than the pKa of Eul-cys polymer. The Eul-cys/GSH NPs obtained were characterized by dynamic light scattering, transmission electron microscopy, and atomic force microscopy. The results obtained showed that the average particle size ranged from 240 to 280 nm, and the particles were almost spherical in shape. The in vitro drug release results showed that the Eul-cys/GSH NPs retained a large amount of insulin in simulated gastric fluid, while a significant insulin release was found in simulated intestinal fluid. The in situ release study suggested that NPs released a greater amount of FITC-insulin (49.2 %) into the intestinal mucus layer compared with that of FITC-insulin solution (16.4 %), which facilitating insulin delivery through the intestinal mucosa. Eul-cys/GSH NPs exhibited promising mucoadhesive properties demonstrated using an in vitro cell model. Consequently, NPs were introduced into the ileum loop of healthy rats, thus enhancing the intestinal absorption of insulin and providing a prolonged reduction in blood glucose levels. These results suggest that Eul-cys/GSH NPs may be a promising delivery system for the treatment of diabetes.

Keywords Mucoadhesive nanoparticles ·
pH-sensitive · Thiolated polymers · Permeation enhancing · Oral drug delivery · Nanomedicine

Y. Zhang · H. Li · H. Sun
Normal College, Shenyang University, Shenyang 110044,
China

Y. Zhang · X. Lin · X. Du · S. Geng · X. Tang (✉)
Department of Pharmaceutics, Shenyang Pharmaceutical
University, No. 103, Wenhua Road, Shenyang 110016,
China
e-mail: tanglab@126.com

Y. Zhang · W. Xiao (✉)
Jiangsu Kanion Pharmaceutical Co., Ltd, No. 58,
Yuankang Road, Lianyungang 222047, China
e-mail: wzhzh-nj@tom.com

Introduction

Oral delivery is an attractive route for the delivery of drugs, due to its convenience and high patient compliance, especially when long term or daily use is required (Gamboa et al. 2013; Bakhru et al. 2013; Lin et al. 2005). However, most biological agents, such as polypeptides and proteins, fail to meet the

requirement for oral delivery because of their poor bioavailability. Pre-systemic enzymatic degradation and poor transmucosal permeability are the major obstacles to efficient oral protein and peptide delivery (Lopes et al. 2014; Ganguly et al. 2014; Chen et al. 2011; Xiong et al. 2013; Zhao et al. 2013). In addition, the mucus layer that lines the surface of the GI tract can present another barrier to delivery and can result in rapid nanoparticle clearance due to the quick cell turnover (Lai et al. 2009). As a major protein drug used to treat diabetes, insulin has been conventionally administered by subcutaneous (SC) injection. Although many attempts have been made to develop an effective oral insulin delivery system, there are still many challenges that need to be addressed before its full clinical potential can be achieved.

In order to improve the oral bioavailability of insulin, a variety of innovative approaches have been developed to tackle these challenges, including the use of small molecule permeation enhancers, enzyme inhibitors, and the encapsulation of protein drugs into microspheres or nanoparticles (Makhlof et al. 2011; Su et al. 2012; Liu et al. 2013; Jain et al. 2012; Yang et al. 2014). The advantages of using nanoparticles include the protection of insulin from degradative enzymes, increased mucoadhesion, and increased retention in the GI tract. Increased mucoadhesion obtained with nanocarriers has the benefit of improving the oral delivery of poorly adsorbed drugs by increasing the time and amount of interaction with the mucus layer of the intestine (Kawashima et al. 2000; Takeuchi et al. 2001). Thus, if a nanoparticle can stick to the mucus layer located beneath the loosely adherent mucus layer on the surface, it has an increased chance of transcellular migration into the lower layers of the epidermal wall, the epithelial layer, and the lamina propria (Ensign et al. 2012). Nanoparticles can have greater mucoadhesive properties with the use of mucoadhesive polymers, which include Eudragit, poly (acrylic acid), sodium alginate, and chitosan (Felber et al. 2012).

Among these materials, pH-sensitive hydrogels are of especial interest from the pharmaceutical point of view, which exhibit reversible formation of inter polymer complexes that are insoluble at lower gastric pH, but swell in alkaline conditions of the intestine, and dissociate the complexes to release insulin. In this category, one of the most widely investigated systems is that of pH-sensitive graft polymers of methacrylic acid. Acrylate and methacrylate copolymers are commercially available as Eudragit polymers in different ionic forms, since these are widely employed in the preparation of microspheres to deliver macromolecules (Attivi et al. 2005; Mundargi et al. 2011).

In this study, thiolated polymeric nanovesicles composed of Eudragit L100-cysteine (Eul-cys) and reduced glutathione (GSH) were designed and prepared. Sulfhydryl modification was achieved by grafting cysteine to the carboxylic acid group of Eudragit L100, and insulin and GSH were embedded into the Eul-cys conjugates to form insulin-loaded Eul-cys/GSH nanoparticles. Here, GSH was served as an absorption enhancer to increase the intestinal uptake and membrane transport of insulin. Because of the presence of numerous thiol groups on the surface, these nanoparticles exhibited excellent mucoadhesive properties and the ability to be retained on freshly excised intestinal mucosa. In order to verify the increased mucoadhesive effect caused by the formation of the disulfide bonds, a comparison was made between the Eul-cys conjugate and unmodified polymer using rheology experiments. The insulin-loaded Eul-cys/GSH NPs were prepared by diffusion partitioning under mild conditions, and they were then characterized in terms of their particle size, zeta potential, and morphology. Moreover, the Eul-cys/GSH NPs were evaluated with respect to the vitro and in situ release of insulin, their mucoadhesive properties, and in vivo biological efficacy after oral administration using healthy rats as a closed ileum-loop model.

Materials and methods

Materials

Porcine insulin (27.8 IU mg^{-1}) was purchased from Xuzhou Wanbang Biochemical Pharmaceutical Co., Ltd, China. Eudragit® L-100 was obtained from Ionic Degussa (China). Reduced glutathione (GSH) was purchased from National Chemical Reagent Co., Ltd, China. L-Cysteine (cys), Porcine gastric mucin, fluorescein isothiocyanate (FITC), pyridinium iodide (PI), and 2-(4-amidinophenyl)-6-indolecarbamidine dihydrochloride (DAPI) were obtained from Sigma, St. Louis, MO, USA, while tris (2-carboxyethyl) phosphine (TCEP) was obtained from Aladdin

Chemistry Co., Ltd, China. All the other reagents were of analytical grade.

Caco-2 cells were obtained from the Institute of Biochemistry and Cell Biology (Shanghai, China). The HT29-MTX cell line was a kind gift from Dr. Thecla Lesuffleur (INSERM, Paris, France). Cells from the 35th–40th passages and 48th–53rd for Caco-2 and HT29-MTX cells, respectively, were used in the present study.

The animal experiments in this work complied with the regulations of the Committee on Ethics in the Care and Use of Laboratory Animals at Shenyang Pharmaceutical University.

Preparation of Eul-cys conjugates

The Eul-cys conjugates were synthesized by the formation of amide bonds between the primary amino groups of cysteine and the carboxylic acid groups of Eudragit L100 mediated by EDC as described by our research group previously (Zhang et al. 2012). The total amount of thiol groups attached to the polymers was quantified by Ellman's reagent and samples with a thiol group content of 396.3 μmol g^{-1} conjugate were used to prepare nanoparticles.

Rheology experiments

Porcine gastric mucin (0.2 g) was hydrated in 2.5 mL of demineralised water under continuous stirring at 4 °C overnight. The pH of the mucin solution was adjusted to 6.8 with 1 M NaOH and then diluted to a final volume of 5 mL with phosphate buffer pH 6.8 (0.2 M). This solution was served as the mucin stock solution (4 %, m/v). Eul-cys and unmodified Eudragit L100 were hydrated in phosphate buffer pH 7.4 to reach a final concentration of 3 % (m/v) and incubated at 37 °C for 30 min. The polymer solutions were added to an equal volume of mucin solution under stirring, and the pH of the mixture was adjusted to 7.4 with 1 M NaOH. After a 30 min incubation, half the sample volume containing polymer/mucin incubates was withdrawn, and a reducing agent TCEP (20 mM) was added followed by a 30 min incubation to split the disulfide bond. Samples containing polymer/mucin and polymer/mucin + TCEP were analyzed using an AR2000 ex Rheometer (Waters, UK). The linear viscoelastic region of each test sample was determined by initial torque sweeps at a frequency of 1 Hz.

Oscillatory tests within the linear viscoelasticity region were performed over a frequency range from 0.1 to 10 Hz, and the frequency dependence of the storage modulus G′ (w) and loss modulus G″ (w) was recorded.

Preparation of insulin-loaded Eul-cys/GSH nanoparticles

Insulin-loaded Eul-cys/GSH NPs were prepared by the diffusion method. First, Eul-cys conjugate (20 mg) was dissolved in deionized water (10 mL) and NaOH (1 M) was added to bring the pH close to 10.0. Sonication (40 Hz, 25 °C) was performed for 60 s, and then insulin solution (5 mL, 1 mg mL^{-1}) was added drop-wise to the polymer solution under gentle stirring, and then GSH solution (2 mg mL^{-1}) was blended into the mixture under stirring (100 rpm). Subsequently, the solution was gradually adjusted to pH 4.8 with 0.02 M hydrochloric acid, and incubated for 15–20 min to form the nanocomplex. The NPs were collected and washed with 2 % trehalose (pH 4.8) by centrifugation at 12,000 rpm for 30 min then lyophilized, and the NPs were stored at 4 °C for further study.

Characterization of NPs

A JEM-2100 transmission electron microscope (TEM) was used to observe nanoparticle morphology. One drop of colloidal suspension was spread onto a carbon-coated copper grid, which was then dried at room temperature for TEM analysis. The size and morphology of the Eul-cys/GSH nanocomplexes were characterized by AFM (CSPM5500, Benyuan, China). Briefly, 1–2 μL of samples containing nanoparticles were deposited on a freshly split untreated mica sheet and allowed to dry at room temperature before imaging. The imaging was performed with a silicon nitride tip in tapping mode allowing AFM to resolve images without damaging the sample surface. The resonant frequency and scan speed was 220 and 0.8–1.1 Hz, respectively.

Effect of GSH on the mucoadhesive properties

Prior to the determination of the mucoadhesive properties, Eul-cys conjugates were labeled with 6-amino-fluorescein (6-AF) through amide bond

formation between the NH_2 on 6-AF and the COOH on Eul-cys as mediated by EDC/NHS at pH 5.0 (Zhang et al. 2012). Then, the resulting 6-AF-Eul-cys and GSH (at a mass ratio of 8:1, 6:1, 4:1 and 2:1, respectively) were allowed to form nanoparticles with insulin as described in the section of preparation of NPs. Subsequently, fasted rats were sacrificed and an jejunum loop of about 10 cm was constructed, which attached to a half pipe placed at an angle of 45° and equilibrated with 100 mM phosphate buffer (PBS, pH 6.8) at 37 °C. NPs were injected onto the intestinal mucosa and continuously rinsed with PBS at a flow rate of 6 mL h^{-1} for 3 h. Then, NPs were scraped off and centrifuged (3,000× rpm) for 5 min, and the supernatant was used for fluorescence analysis. (λ_{EX}: 485 nm, λ_{EM}: 525 nm).

In vitro drug release

In order to simulate the stomach and intestinal environments, insulin release from Eul-cys/GSH NPs was performed in solutions of pH 1.2 HCl (Simulated Gastric Fluid, SGF) and pH 7.4 PBS buffer (Simulated Intestinal Fluid, SIF), respectively. The formulations were kept in pH 1.2 HCl for the first 2 h and, later, in pH 7.4 PBS to simulate the intestinal environment. Briefly, NPs (1 mL) were withdrawn and centrifuged (15,000 rpm, 20 min), the supernatants were discarded and then the NPs were dispersed in pH 1.2 HCl under continuous oscillation (100 rpm, 2 h) at 37 °C. The release medium was replaced with pH 7.4 PBS for further 4 h dissolutions. At appropriate intervals, NPs were centrifuged and the supernatants (0.2 mL) were withdrawn and replaced with fresh media. The release samples were filtered and analyzed using HPLC. The chromatographic conditions were the same as those described by our group previously (Zhang et al. 2012).

Circular dichroism (CD)

Conformational changes of insulin released from Eul-cys/GSH NPs were evaluated by circular dichroism. The dissolution media were subjected to ultracentrifugation and the supernatant containing released insulin were collected for CD analysis. All samples were measured by scanning from 200 to 250 nm on a CD spectropolarimeter (Jasco J-810, japan) on a 1-cm path length quartz cell at protein concentration of 1 mg mL^{-1}. Analysis conditions were used: 0.5-nm bandwidth, 10-mdeg sensitivity, 0.2-nm resolution, 2-s response, and 10-nm min^{-1} scanning speed. The buffer baseline was subtracted from the average spectra.

In situ drug release in rat ileum

FITC-insulin was prepared as described by a previous report (Li et al. 2007). Rats were fasted overnight then anesthetized by an intraperitoneal injection of trichloroacetaldehyde hydrate (350 mg kg^{-1} body weight), and a midline incision was made in the abdomen. For the assessment of in situ FITC-insulin release, an ileal sac (about 6 cm in length) was constructed by tying both ends of the segment, followed by the injection of 1 mL FITC-insulin-loaded Eul-cys/GSH NPs (10 mg mL^{-1}) saline solution. Following incubation in the abdominal cavity for 4 h, the sac was excised and the fluid was collected, followed by centrifugation at 12,000 rpm for 10 min and the FITC-insulin was determined in the supernatant. The mucus layer was then scraped off, homogenized with cold saline, and centrifuged at 12,000 rpm for 10 min. The amount of FITC-insulin in the supernatant was quantified and taken to be the amount adhering to the mucosa.

Cell adhesion

Caco-2 and HT29 cells were grown separately in flasks in DMEM supplemented with 10 % (v/v) fetal bovine serum, 1 % (v/v) non-essential aminoacids, 1 % (v/v) L-glutamine and 1 % (v/v) penicillin and streptomycin, at 37 °C under a 5 % CO_2 water saturated atmosphere. When the cell monolayer reached 80 % confluence, cells were harvested from the flasks with trypsin–EDTA and a predetermined amount of cells of each type were mixed prior to seeding to yield cell ratios of 1:1 for Caco-2 (3×10^4 cells) to HT29 cells, and cultured on glass cover slips placed in 6-well cell culture plates. Then, after 3–4 days post-seeding, the medium was replaced with HBSS-HEPES (buffered at pH 7.2 with 30×10^{-3} M HEPES), and 0.5 mL 6-amino-fluorescein labeled Eul-cys/GSH NPs (the method of synthesis has been reported by us previously (Zhang et al. 2012) at a concentration of 1 mg mL^{-1} was added followed by incubation of the cells. At predetermined times, the cells were rinsed with HBSS, and fixed with 4 %

paraformaldehyde. Then, 300 μL PI (5 μg mL^{-1}) solution was added to the co-cultured cells to label the cell nuclei and followed by incubation for 10 min at 37 °C. The samples were rinsed twice with HBSS and mounted for examination by fluorescence microscopy.

Absorption in situ loop

Sprague–Dawley rats, weighing approximately 180–220 g, were fasted for 24 h prior to the experiments and were anesthetized by an i.p. injection of 50 mg kg^{-1} sodium pentobarbital. In this study, the in situ loop method was employed as described previously (Morishita et al. 2004; Nakamura et al. 2004). Briefly, a front middle incision was made in the abdomen and the ileal segment was isolated. A 10-cm section of the isolated segment was washed with 20 mL PBS at 37 °C, and the both ends of the segments were tightly closed. Rats were left on the board at 37 °C for 1 h to allow them to recover from the elevated blood glucose levels. The formulations (insulin, insulin-loaded Eul-cys NPs and insulin-loaded Eul-cys/GSH NPs) were suspended in 2 mL PBS in a syringe and infused into the above ileal segment, and the dose for all samples was fixed at 50 IU kg^{-1} body weight. During the experiment, 0.2 mL aliquots of blood were taken from the jugular vein at $t = 0, 0.25, 0.5, 1, 2, 3, 4, 6,$ and 8 h after dosing. The blood glucose levels were determined using an ACCU-CHEK Performa® glucometer (Roche, Germany).

Statistical analysis

The results are expressed as mean ± standard deviation (S.D.). Values from different groups were compared with the control groups using Student's t test. A difference was considered to be statistically significant when the P value was less than 0.05.

# Results and discussion

Rheology measurements

Representative examples of the viscoelastic profiles of the polymer-mucin solutions and polymer-mucin + TCEP solutions are given in Fig. 1. As seen from Fig. 1a, c, there is increase in the viscoelastic moduli G′ and G″ of thiolated polymer-mucin mixture

compared with unmodified polymer-mucin. Such rheological profiles would be expected for the inter-molecular interaction due to the formation of disulfide bonds between the Eul-cys and the mucin layer. In order to verify the role of the disulfide bond, the viscoelasticity was also measured in the presence of TCEP, a small molecule which is capable of reducing disulfide bonds. As can be seen from the results in Fig. 1b, d, addition of TCEP reduces the viscosity of all samples, but to different degrees. As expected, adding TCEP to the Eul-cys/mucin mixture led to a much more significant reduction in G′ and G″. This suggests that the viscosity changes due to the presence of TCEP which is an outcome of reduction and breakage of the disulfide bridges which are initially present both in Eul-cys solutions and Eul-cys/mucin mixtures. These observations support the assumption that disulfide bridges could potentially increase the ability of mucoadhesive polymers such as Eul-cys to interact with the mucus surface. Further evidence that such a covalent bond between thiol and mucus is responsible for the enhanced mucoadhesive properties, and viscosity is given by unmodified Eudragit L100 which has no thiol-bearing side chains and, therefore, exhibits little change in viscoelastic properties after TCEP treatment.

Preparation and characterization of NPs

Because the drug solution was loaded into the NPs by diffusion, a higher swelling ratio would lead to a higher loading efficiency. Therefore, insulin loading into the NPs was performed by premixing insulin HCl solution with alkaline polyanion solutions, which led to a slow reduction in pH. Following the slow addition of insulin solution, the polyanion solution spontaneously changed from clear to opalescent and, finally, to a turbid suspension, indicating the formation of nanoparticles and eventually aggregates. The NPs were produced at a Eul-cys concentration of 0.2 % (w/v) and a preparation pH of 4.8, therefore, insulin and GSH change from the anionic to cationic form when the pH is below their PI (PI $_{insulin}$: 5.3 and PI $_{GSH}$: 5.9). The formation of self-assembled Eul-cys/GSH NPs relies on its ability to gel spontaneously on contact with polyanion solutions as a result of inter- and intra-molecular cross-linking between positively charged insulin/GSH and negatively charged polyanions, as shown in Fig. 2a. The synthesis of nanoparticles by

Fig. 1 The dynamic oscillation spectra for 3 % Eul-cys and Eul mixtures with 4 % mucin and polymer/mucin mixtures with 20 mM TCEP. **a** Eul/mucin **b** Eul/mucin +TCEP **c** Eul-cys/mucin **d** Eul-cys/mucin +TCEP
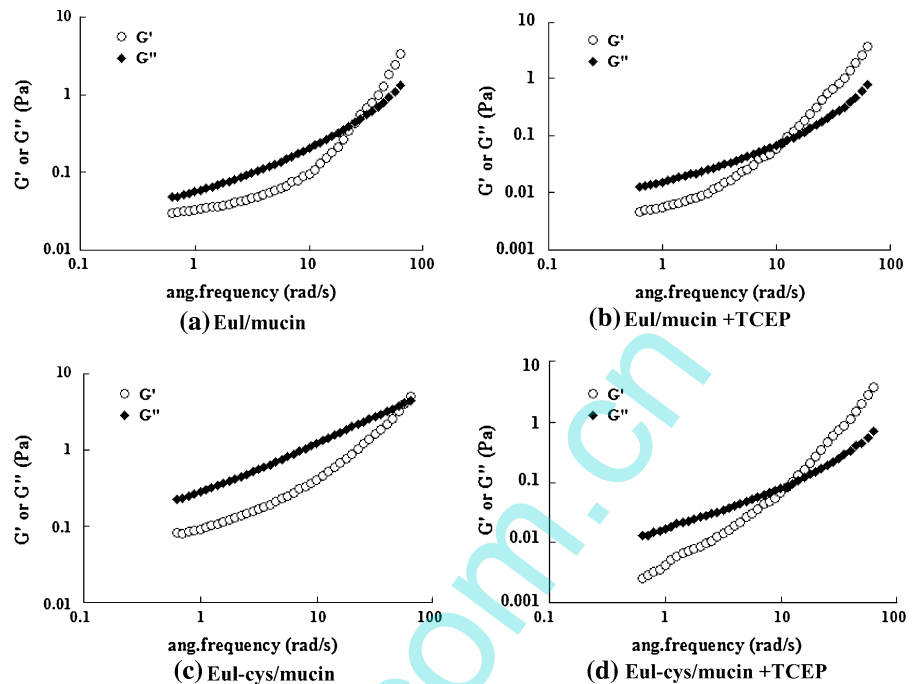
equilibrium partitioning under mild conditions resulted in NPs with an average diameter of 240–280 nm, negative charges (-3.1 ± 0.9 mV), with a PI of 0.215, measured by dynamic light scattering. Figure 2b shows a representative transmission electron micrograph of Eul-cys/GSH NPs that clearly indicates the formation of well-defined spherical particles with a smooth surface. AFM images of Eul-cys/GSH nanoparticles are shown in Fig. 2c. Particles have an approximately spherical shape, which is similar to the TEM image. Observation of the samples by TEM and AFM suggests that insulin was able to penetrate into the Eul-cys/GSH nanoparticles and form a nanocomplex.

Effect of GSH on the mucoadhesive properties

GSH, a small peptide molecule, is capable of opening the cellular tight junctions in combination with thiolated polymers to achieve increased intestinal absorption of biomacromolecules, such as insulin. However, it might exchange its sulfhydryl group present in cysteine residues with a disulfide bond formed by Eul-cys NPs with the mucus gel layer, which then leads to a reduced bioadhesion of NPs and detachment from the intestinal mucosa. As a consequence, GSH should be in a suitable ratio with the

thiomer in the thiolated delivery system. As shown in Fig. 3, an obvious reduction in mucoadhesive properties of Eul-cys NPs appeared when the mass ratio of GSH and Eul-cys conjugate was above 1:2 (near 33 % for GSH), which was a significantly higher tolerance level on GSH than in a previous study involving chitosan-TBA and GSH tablets (15 % GSH) reported by Bernkop-Schnurch et al. (2004). This may be explained by different dosage forms and evaluation methods of the mucoadhesive properties. Nanoparticles have a higher surface area than tablets, resulting a closer and stronger contact with the intestinal mucosa and less influence by GSH. Hence, in Fig. 3, a mass ratio of GSH and Eul-cys (1:4, 20 % for GSH) not only provide an improved permeation enhancing effect but there was also no effect on the mucoadhesive properties of the NPs.

In vitro release study

The release of insulin and GSH from pH-sensitive Eul-cys/GSH NPs was monitored at different pH values as a function of time. Insulin and GSH release was partially inhibited in pH 1.2 HCl solution, and a rapid release was noted after being transferred to pH 7.4 PBS. The cumulative release of the encapsulated insulin within 4 h in pH 7.4 PBS was 85 % in

Fig. 2 Schematic representation of self-assembled Eul-cys/GSH NPs and drug release mechanisms from NPs (**a**), TEM (**b**), and AFM (**c**) images of Eul-cys/GSH NPs
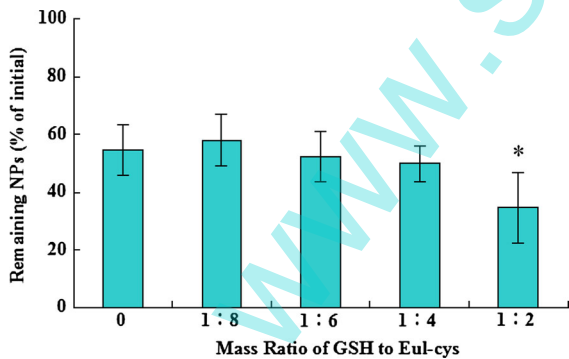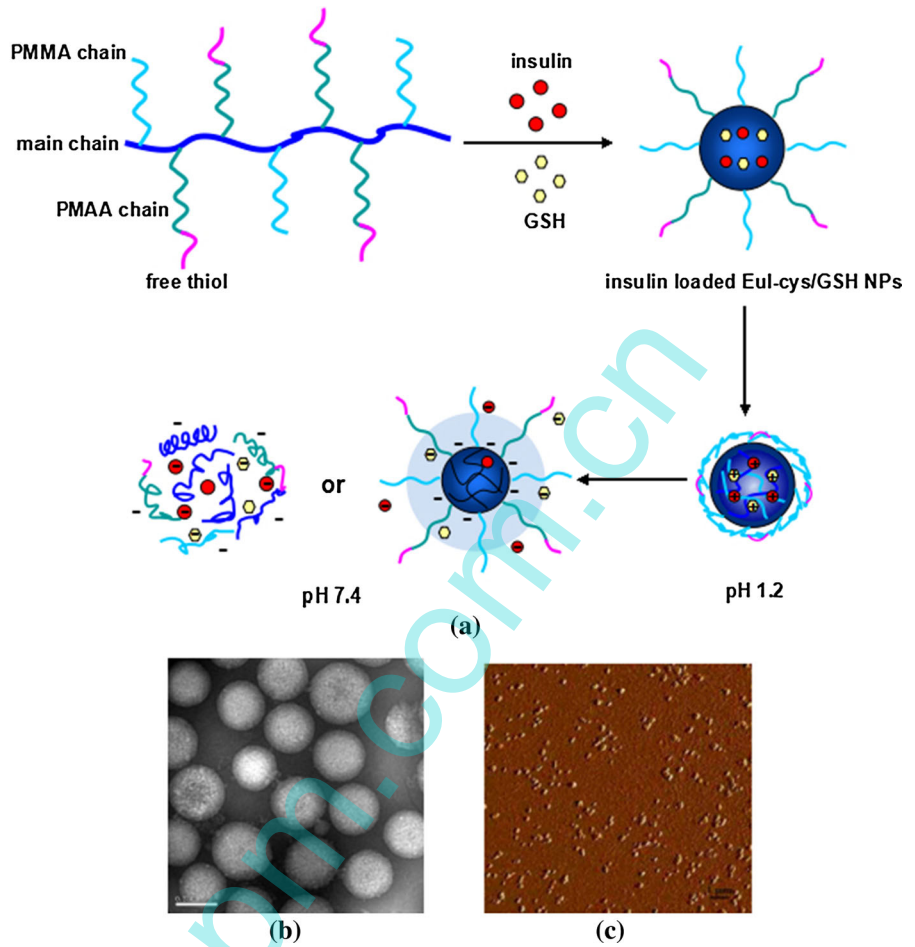

Fig. 3 Influence of GSH on the mucoadhesive properties of Eul-cys NPs. Mucoadhesion were evaluated via 6-AF labeled NPs on freshly excised rat intestinal mucosa rinsed with 100 mM phosphate buffer (pH 6.8) at 37 °C. Indicated values are means of at least three experiments ± S.D. *Asterisk* differs from Eul-cys NPs without GSH, $P < 0.01$

comparison with 20 % in HCl solution. The increased release rate with the increase in medium pH is believed to be caused by an increase in the swelling ratio of NPs. Under acidic conditions, as shown in Fig. 2a, the NPs collapsed quickly, and the diffusion of insulin was blocked by the dense hydrogel networks. However, in neutral SIF, insulin release in vitro exhibited a markedly rapid initial burst release of 40 % in 30 min, followed by a slower release of 80 % in 4 h, due to the corresponding increased swelling ratios of NPs in phosphate buffer at pH 7.4. In addition, the observed burst release may also be related to the surface adsorption of insulin and electrostatic repulsion between polymers and insulin (Zhang et al. 2014). What is interesting, among the strategies used to increase the bioavailability, NPs are

not a delivery system in terms of controlled release, and insulin absorption could still be promoted by polymer mucoadhesion, which can produce a microclimate diffusion gradient favorable for drug absorption (Deat-Laine et al. 2012; George and Abraham 2006). It can be also seen that there was a faster release of GSH than insulin in neutral SIF illustrated in Fig. 4. GSH has been shown to be capable of opening tight junctions by inhibiting PTP activity, which may increase insulin delivery by paracellular transport.

Secondary structural conformation analysis (CD)

To determine the secondary structural conformation changes of insulin before and after self-assembly process, circular dichroism (CD) spectra were collected and analyzed. It can be found that in the far-UV region (Fig. 5), there are two major negative maximal bands at 208 and 222 nm, which are assigned to the contribution of α-helical and β-sheet structure, respectively. It is suggested that negligible changes in band intensity at 208 and 222 nm were found in insulin after the loading process and no significant difference in the secondary structure of released insulin compared to native insulin.

In situ drug release

Due to the covalent attachment of cysteine hydrochloride, the polymeric NPs exhibited increased
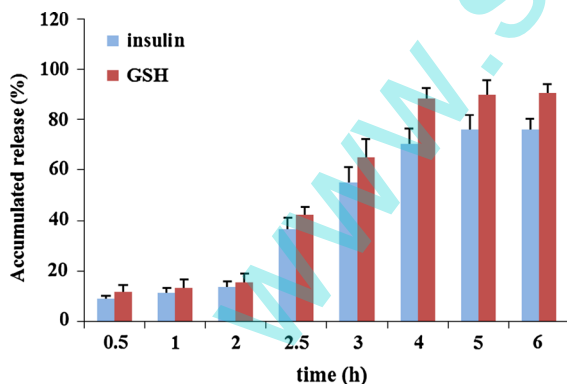
mucoadhesive properties. In accordance with their stronger mucoadhesive capacities, NPs were more potent in releasing larger amounts of the encapsulated FITC-insulin into the intestinal mucus layer while smaller amounts were released into the lumen, in contrast with the solution group, as shown in Fig. 6. This was advantageous for the absorption of insulin, because the numbers of enzymes are less in the intestinal mucus layer than in the lumen, and the degradation of insulin was reduced for the NPs compared with the administration of insulin solution.

Cell adhesion

In vitro cell culture models for screening and predicting the potential success of a novel oral drug candidate have become a routine part of drug discovery and development. A variety of cell monolayer models that mimic the human intestinal epithelial barrier have been developed
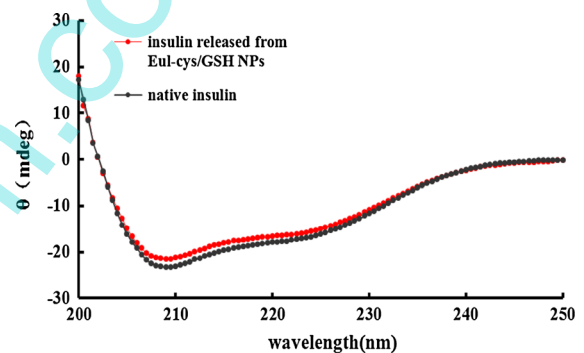
Fig. 5 Far-UV circular dichroism of release insulin from Eul-cys/GSH NPs, and the untreated native insulin was set as control

Fig. 4 In vitro release process of insulin and GSH from Eul-cys/GSH NPs at HCl solution (pH 1.2) in first 2 h and at pH 7.4 PBS in the following 4 h, simulating the pH environments changes from the fasting stomach to the intestine (duodenum and jejunum), the *blue color* represents insulin release from Eul-cys/GSH NPs, the *red color* represents GSH release from Eul-cys/GSH NPs. Indicated values were mean ± S.D. ($n = 3$). (Color figure online)
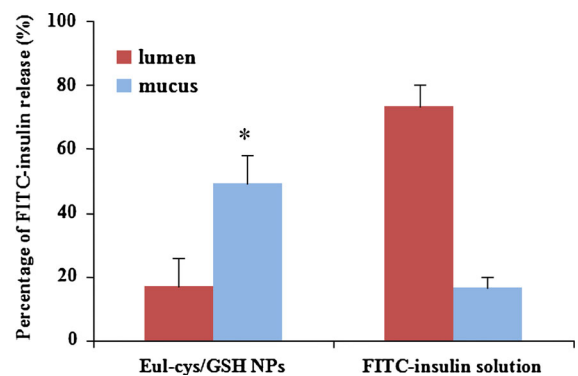
Fig. 6 In situ FITC-insulin release from Eul-cys/GSH NPs in rat intestinal lumen and mucus. Indicated values were mean ± S.D. ($n = 3$)

and provide an ideal system for the rapid assessment of the intestinal permeability of new drug candidates. Among the cell culture models, the Caco-2 cell line is the most widely used and best characterized system. However, the Caco-2 monolayer model still lacks important properties that make further refinement desirable. For example, they represent the tightness of the junctions present in the colon, as opposed to the looser junctions present in the small intestine. Also, the Caco-2 model lacks mucus-producing cells, the second most frequent cell type. Thus, co-culture of Caco-2 cells with goblet and mucus-secreting cell characteristics such as HT29-MTX cells has been proposed in order to solve this problem. The presence of HT29-MTX cells in the co-culture reduced the overall resistance of the cellular monolayer and, thus, the cellular resistance values more closely mimicked the in vivo small intestinal resistance values. In this study, the interaction between Eul-cys/GSH NPs and co-cultured cells as a function of the incubation time is shown in Fig. 7. As expected, the green fluorescence in the cells grew stronger over time and, in particular, there was increased fluorescence in the intercellular space region. The results obtained suggest that thiomer-based nanoparticles work as permeation enhancers that transiently open epithelial tight junctions (paracellular route) and consequently increase intestinal permeability, which is a promising approach to overcome poor oral macromolecule permeability.

The transport of insulin across Caco-2 and Caco-2/HT29-MTX co-culture monolayers has been previously reported, and it was found that there was a rise in cumulative insulin transport in the co-culture when compared with the monoculture model (Woitiski et al. 2011). The increase in insulin permeability in the Caco-2/HT29-MTX co-culture model was closely related to the reduction in tight junction stickiness, promoting the paracellular transport of insulin. Moreover, insulin is released from Eul-cys/GSH NPs in a pH-dependent manner under simulated gastrointestinal conditions, while the release at gastric pH is almost avoided, allowing a continuous release at an intestinal pH up to 4 h. The mucus layer produced by HT29 cells retains nanoparticles closer to the potential sites of permeation for longer periods of time, and the enzymatic degradation ratio of insulin was reduced significantly, which also contributed to the increased absorption of insulin. Therefore, the mucoadhesive properties and permeation enhancing effect of the thiomer-GSH system may have contributed significantly to the increased insulin permeation, which was also observed here.

Absorption in situ loop

Previously, it has been reported that the oral administration of insulin-loaded Eul-cys NPs could significantly reduce the blood glucose levels in diabetic rats (Zhang et al. 2012). The focus of this work was to prepare complexation NPs containing a small tripeptide GSH and to evaluate how the thiomer–GSH drug delivery system affected the blood glucose levels of healthy rats following direct intestinal administration using a closed-loop model. The glucose response and insulin absorption profiles are shown in Fig. 8. No hypoglycemic effect or insulin absorption was observed if insulin solutions were applied alone. Insulin-loaded Eul-cys/GSH NPs have a significant and dose-dependent hypoglycemic effect compared with insulin solution, indicating that there is appreciably increased insulin absorption by this carrier from the ileal segments. Their relative pharmacological bioavailability (PA %) of Eul-cys/GSH after enteral administration at the dose of 25 and 50 IU kg^{-1} was estimated as 3.2–7.4 %. It should be noted that the ileal insulin absorption from NPs occurred rapidly, due to the avoidance of oral transport and NPs swelled quickly and, so, instantly released drug under neutral and basic conditions. The potential mechanism associated with the hypoglycemic effect may be attributed to several factors: (1) Thiolated polymeric NPs are in close contact with the mucus layer, leading to a prolonged retention time in the intestine, as a result of opening of the tight junctions of the epithelial cells, and the insulin absorption through the intestinal epithelium is increased. (2) GSH is able to inhibit protein tyrosine phosphatases (PTP), which results in closing of the tight junctions due to the dephosphorylation of occludin protein (Clausen et al. 2002). An additional synergistic effect can be attributed to the thiol groups grafted onto the NP surface to reduce the formation of GSSG (oxidized form) thereby increasing the amount of GSH at the apical surface in the gastrointestinal mucosa. (3) Peyer's patches are the primary induction sites for oral delivery of colloidal particulates with an optimal particle size of 200–300 nm (Desai et al. 1996). In the current investigation, the diameter of the test nanoparticles was 250 nm, thus inducing a stronger uptake by M cells and a significant
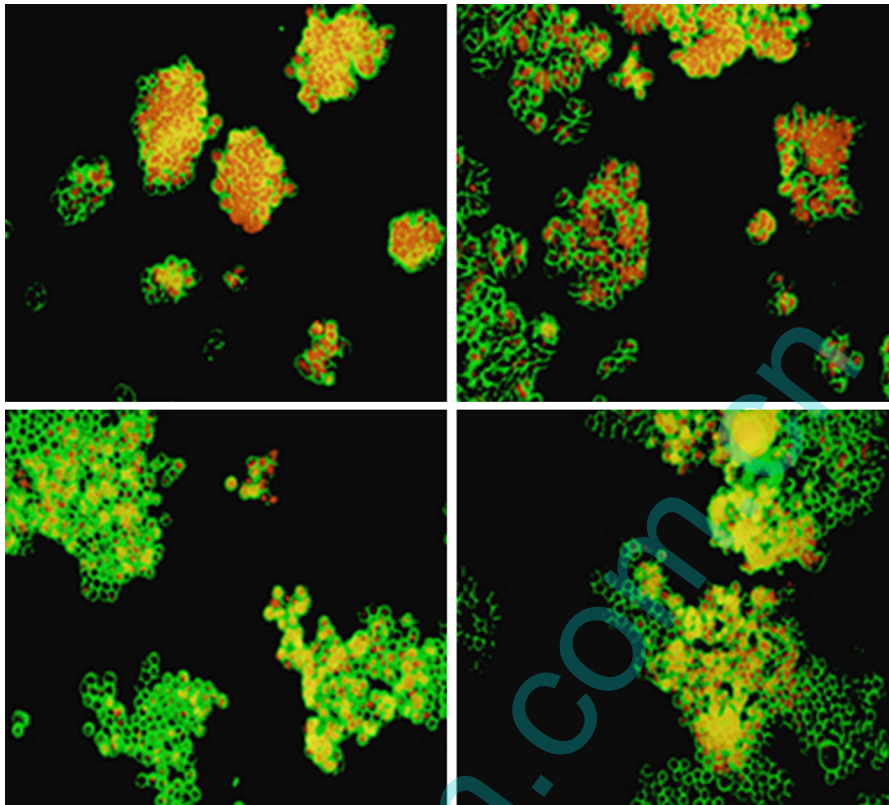
Fig. 7 Association of 6-amino-fluorescein labeled Eul-cys/GSH NPs with Caco-2/HT29-MTX co-cultured cells, *green* 6-amino-fluorescein, *red* PI stained cell nuclei. Fluorescent images of cell uptake as a function of incubation time (0.5, 1, 2, and 3 h). (Color figure online)
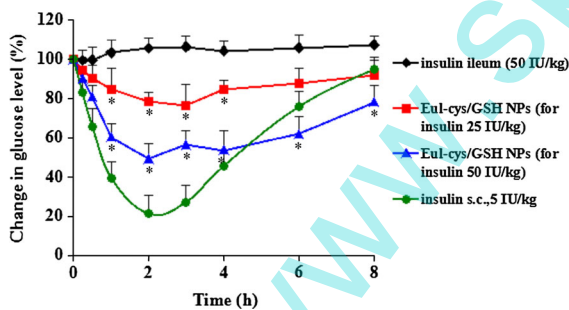

Fig. 8 Serum glucose levels following the ileal administration of insulin solution (50 IU/kg), insulin-loaded Eul-cys/GSH NPs to normal rats at a dose of 25 and 50 IU kg^{-1}. Subcutaneous administration of insulin solution (5 IU kg^{-1}) was used as positive control. Each data represents the mean $\pm$ S.D. of five animals per group. Significant difference from insulin solution: $P < 0.05$

pharmacological effect. These results have proved that Eul-cys combined with GSH were able to effectively deliver biologically active insulin via the oral route.

Conclusion

In the present study, Eul-cys/GSH vesicles were prepared as a carrier for the oral delivery of insulin. The rheological experiment confirmed that the excellent mucoadhesive properties of the thiolated polymer were attributed to the presence of an intermolecular interaction, such as disulfide bridges, between the polymer chains and glycoprotein in the mucin. The in vitro drug release results revealed that the release of insulin and GSH from Eul-cys/GSH NPs was markedly reduced in SGF, while it was increased significantly in SIF. The in vitro cell model proved that Eul-cys/GSH NPs have promising mucoadhesive properties. In vivo evaluation using an ileal closed-loop model in rats showed that the blood glucose level of rats could be effectively reduced after intestinal administration of Eul-cys/GSH. It was found that the blood glucose concentration decreased immediately and the highest blood glucose reduction was achieved after about 2 h

at an insulin dose of 50 IU kg^{-1}. Furthermore, the blood glucose concentration increased slowly and maintained the hypoglycemic effect for at least 8 h. Therefore, the Eul-cys/GSH vesicles are promising polymeric carriers for the oral delivery of insulin.

References

Attivi D, Werhle P, Maincent P et al (2005) Formulation of insulin-loaded polymeric nanoparticles using response surface methodology. Drug Dev Ind Pharm 31:179–189

Bakhru SH, Furtado S, Morello AP et al (2013) Oral delivery of proteins by biodegradable nanoparticles. Adv Drug Deliv Rev 65:811–821

Bernkop-Schnurch A, Guggi D, Pinter Y (2004) Thiolated chitosans: development and in vitro evaluation of a mucoadhesive, permeation enhancing oral drug delivery system. J Control Release 94:177–186

Chen MC, Sonaje K, Sung HW et al (2011) A review of the prospects for polymeric nanoparticle platforms in oral insulin delivery. Biomaterials 32:9826–9838

Clausen A, Kast C, Bernkop-Schnurch A (2002) The role of glutathione in the permeation enhancing effect of thiolated polymers. Pharm Res 19:602–608

Deat-Laine E, Hoffart V, Beyssac E et al (2012) Development and in vitro characterization of insulin loaded whey protein and alginate microparticles. Inter J Pharm 439:136–144

Desai M, Labhasetwar V, Levy R et al (1996) Gastrointestinal uptake of biodegradable microparticles: effect of particle size. Pharm Res 13:1838–1845

Ensign LM, Cone R, Hanes J (2012) Oral drug delivery with polymeric nanoparticles: The gastrointestinal mucus barriers. Adv Drug Deliv Rev 64:557–570

Felber AE, Dufresne MH, Leroux JC (2012) pH-sensitive vesicles, polymeric micelles, and nanospheres prepared with polycarboxylates. Adv Drug Deliv Rev 64:979–992

Gamboa JM, Leong KW et al (2013) In vitro and in vivo models for the study of oral delivery of nanoparticles. Adv Drug Deliv Rev 65:800–810

Ganguly K, Chaturvedi K, Aminabhavi TM et al (2014) Polysaccharide-based micro/nanohydrogels for delivering macromolecular therapeutics. J Control Release 193:162–173

George M, Abraham TE (2006) Polyionic hydrocolloids for the intestinal delivery of protein drugs: alginate and chitosan—a review. J Control Release 114:1–14

Jain S, Rathi VV, Godugu C et al (2012) Folate-decorated PLGA nanoparticles as a rationally designed vehicle for the oral delivery of insulin. Nanomedicine 7:1311–1337

Kawashima Y, Yamamoto H, Kuno Y et al (2000) Mucoadhesive DL-lactide/glycolide copolymer nanospheres coated with chitosan to improve oral delivery of elcatonin. Pharm Dev Technol 5:77–85

Lai SK, Wang YY, Hanes J (2009) Mucus-penetrating nanoparticles for drug and gene delivery to mucosal tissues. Adv Drug Deliv Rev 61:158–171

Li M, Lu W, Zhang Q et al (2007) Distribution, transition, adhesion and release of insulin loaded nanoparticles in the gut of rats. Int J Pharm 329:182–191

Lin YH, Chung CK, Sung HW et al (2005) Preparation of nanoparticles composed of chitosan/poly-γ-glutamic acid and evaluation of their permeability through Caco-2 cells. Biomacromolecules 6:1104–1112

Liu Y, Kong M, Chen XG et al (2013) Biocompatibility, cellular uptake and biodistribution of the polymeric amphiphilic nanoparticles as oral drug carriers. Colloids Surf B 103:345–353

Lopes MA, Abrahim BA, Ribeiro AJ et al (2014) Intestinal absorption of insulin nanoparticles: Contribution of M cells. Nanomedicine 10:1139–1151

Makhlof A, Tozuka Y, Takeuchi H (2011) Design and evaluation of novel pH-sensitive chitosan nanoparticles for oral insulin delivery. Eur J Pharm Sci 42:445–451

Morishita M, Goto T, Lowman AM et al (2004) Mucosal insulin delivery systems based on complexation polymer hydrogels: effect of particle size on insulin enteral absorption. J Control Release 97:115–124

Mundargi RC, Rangaswamy V, Aminabhavi TM (2011) pH-Sensitive oral insulin delivery systems using Eudragit microspheres. Drug Dev Ind Pharm 37:977–985

Nakamura K, Murray RJ, Lowman AM (2004) Oral insulin delivery using P(MAA-g-EG) hydrogels: effects of network morphology on insulin delivery characteristics. J Control Release 95:589–599

Su FY, Lin KJ, Sung HW et al (2012) Protease inhibition and absorption enhancement by functional nanoparticles for effective oral insulin delivery. Biomaterials 33:2801–2811

Takeuchi H, Yamamoto H, Kawashima Y (2001) Mucoadhesive nanoparticulate systems for peptide drug delivery. Adv Drug Deliv Rev 47:39–54

Woitiski CB, Sarmento B, Veiga F (2011) Facilitated nanoscale delivery of insulin across intestinal membrane models. Int J Pharm 412:123–131

Xiong XY, Li QH, Gong YC et al (2013) Pluronic P85/poly(lactic acid) vesicles as novel carrier for oral insulin delivery. Colloids Surf B 111:282–288

Yang Y, Wang SP, Chen MW et al (2014) Advances in self-assembled chitosan nanomaterials for drug delivery. Biotechnol Adv 32:1301–1316

Zhang Y, Du X, Tang X et al (2014) Thiolated Eudragit based nanoparticles for oral insulin delivery: preparation, characterization, and evaluation using intestinal epithelial cells in vitro. Macromol Biosci 14:842–852

Zhang Y, Wu X, Tang X et al (2012) Thiolated Eudragit nanoparticles for oral insulin delivery: preparation, characterization and in vivo evaluation. Int J Pharm 436:341–350

Zhao X, Shan C, Li R et al (2013) Preparation, characterization, and evaluation in vivo of Ins-SiO2-HP55 (insulin-loaded silica coating HP55) for oral delivery of insulin. Int J Pharm 454:278–284